

High Spin Co(I): High-Frequency and -Field EPR Spectroscopy of $\text{CoX}(\text{PPh}_3)_3$ (X = Cl, Br)

J. Krzystek,[†] Andrew Ozarowski,[†] S. A. Zvyagin,[‡] and Joshua Telser^{*,§}

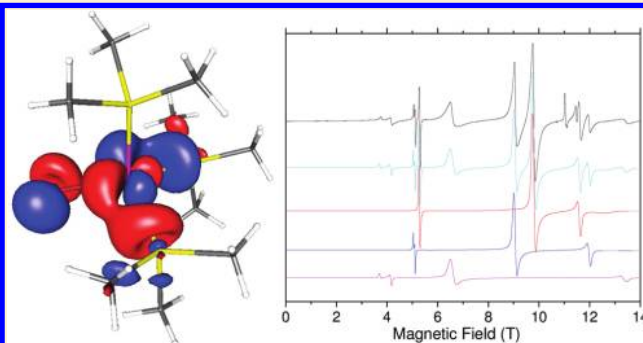
[†]National High Magnetic Field Laboratory (NHMFL), Florida State University, Tallahassee, Florida 32310, United States

[‡]Dresden High Magnetic Field Laboratory (HLD), Helmholtz-Zentrum Dresden-Rossendorf (HZDR), 01314 Dresden, Germany

[§]Department of Biological, Chemical and Physical Sciences, Roosevelt University, Chicago, Illinois 60605, United States

Supporting Information

ABSTRACT: The previously reported pseudotetrahedral Co(I) complexes, $\text{CoX}(\text{PR}_3)_3$, where R = Me, Ph, and chelating analogues, and X = Cl, Br, I exhibit a spin triplet ground state, which is uncommon for Co(I), although expected for this geometry. Described here are studies using electronic absorption and high-frequency and -field electron paramagnetic resonance (HFEPR) spectroscopy on two members of this class of complexes: $\text{CoX}(\text{PR}_3)_3$, where R = Ph and X = Cl and Br. In both cases, well-defined spectra corresponding to axial spin triplets were observed, with signals assignable to three distinct triplet species, and with perfectly axial zero-field splitting (zfs) given by the parameter $D = +4.46, +5.52, +8.04 \text{ cm}^{-1}$, respectively, for $\text{CoCl}(\text{PPh}_3)_3$. The crystal structure reported for $\text{CoCl}(\text{PPh}_3)_3$ shows crystallographic 3-fold symmetry, but with three structurally distinct molecules per unit cell. Both of these facts thus correlate with the HFEPR data. The investigated complexes, along with a number of structurally characterized Co(I) trisphosphine analogues, were analyzed by quantum chemistry calculations (both density functional theory (DFT) and unrestricted Hartree–Fock (UHF) methods). These methods, along with ligand-field theory (LFT) analysis of $\text{CoCl}(\text{PPh}_3)_3$, give reasonable agreement with the salient features of the electronic structure of these complexes. A spin triplet ground state is strongly favored over a singlet state and a positive, axial D value is predicted, in agreement with experiment. Quantitative agreement between theory and experiment is less than ideal with LFT overestimating the zfs, while DFT underestimates these effects. Despite these shortcomings, this study demonstrates the ability of advanced paramagnetic resonance techniques, in combination with other experimental techniques, and with theory, to shed light on the electronic structure of an unusual transition metal ion, paramagnetic Co(I).



INTRODUCTION

Cobalt in the 1+ formal oxidation state ($3d^8$) is relatively uncommon compared to both Co(II) and Co(0).¹ Cobalt(I) is found in one of redox forms relevant in the reaction pathway of cobalamin-dependent enzymes.² In these systems, however, square planar or square pyramidal Co(I) is diamagnetic ($b_2^2e^4a_1^2b_1^0$), as is usually the case for the far more numerous isoelectronic Ni(II) coordination complexes. Organometallic, monocyclopentadienyl Co(I) complexes, such as $\text{CpCo}(\text{CO})_2$ and its derivatives,¹ which are of interest as catalysts for alkyne dimerization³ are diamagnetic, too. There is, however, a bisarene Co(I) complex which is paramagnetic, with an $S = 1$ ground state.⁴ Very recently, a remarkable two-coordinate Co(I) “NacNac” (β -diketiminate) complex, $\text{L}^{\text{tBu}}\text{Co}$ (where $\text{L}^{\text{tBu}} = 2,2,6,6\text{-tetramethyl-3,5-bis}(2,4,6\text{-triisopropylphenylimido)-hept-4-yl}$) with an $S = 1$ ground state has been reported by Holland and co-workers.⁵ Lastly, and of most relevance here, there exist Co(I) complexes with other ligands, such as isonitriles and phosphines. Most have trigonal bipyramidal geometry and are thus diamagnetic. Examples are *trans*- $\text{CoH}(\text{CO})(\text{PPh}_3)_3$ ⁶

and $\text{HCo}[\text{R}^1\text{OP}(\text{OR}^2)_2]_4$ ($\text{R}^{1,2} = \text{Me, Et, etc.}$), which is of interest as a chemical vapor deposition (CVD) precursor.⁷ There are, however, a few which, by virtue of their bulky phosphine ligands, are tetrahedral, and should yield a $^3\text{T}_1(\text{F})$ (orbital and spin triplet; $e^4t_2^4$) ground state. The best known among these is the series $\text{CoX}(\text{PPh}_3)_3$, where X = Cl, Br, I, reported by Aresta et al. in 1969.⁸ The tetrahedral structure was proposed mainly on the basis of the $S = 1$ ground state found for these complexes by magnetometry and was confirmed for the chlorido complex only more than 20 years later by Cassidy and Whitmire;⁹ no structures have been reported for the bromido and iodido analogues. Not long after the report on the PPh_3 complexes, analogous $S = 1$ complexes, $\text{CoX}(\text{PMMe}_3)_3$, where X = Cl, Br, I, were reported by Klein and Karsch,¹⁰ and the structures of the chlorido^{11,12} and iodido,¹³ but not bromido, complexes were shown to be tetrahedral. Two Co(I) complexes with tripodal ligands, in one case triphos (1,1,1-tris((diphenylphosphino)methyl)ethane)^{14,15} and in the other

Received: October 9, 2011

Published: April 6, 2012



tris(2-(diphenylphosphino)ethyl)amine (in which the amino N is not coordinated to Co(I)),¹⁶ have also been shown to be pseudotetrahedral and, correspondingly, have triplet ground spin states.

Over the past years, we have been investigating the electronic structure of paramagnetic transition metal ion complexes with $S > 1/2$ ground states, primarily by high-frequency and γ -field electron paramagnetic resonance (HFEPR) spectroscopy.^{17–19} In particular, the Co(II) ($S = 3/2$) complex series $\text{CoX}_2(\text{PPh}_3)_2$, where X = Cl, Br, I, was investigated, although to date only the chlorido complex has proven tractable to study.²⁰ The analogous Ni(II) ($S = 1$) series, $\text{NiX}_2(\text{PPh}_3)_2$, has been studied more extensively.^{21,22} Consequently, we have turned our attention to a complementary complex of the same general type, namely $\text{CoX}(\text{PPh}_3)_3$, which would allow a comparison between both Co(I) and Co(II) and between Co(I) and Ni(II) in similar coordination environments. The electronic structure of tetrahedrally coordinated Co(II) and Ni(II) is relatively well studied, while that of Co(I) has been barely studied at all. In this study, we have therefore employed ligand-field theory (LFT) and quantum chemical theory (QCT), including both density functional theory (DFT) and unrestricted Hartree–Fock (UHF) computational methods, to shed light on the nature of tetrahedrally coordinated Co(I) systems.

There is, however, another reason for interest in $\text{CoX}(\text{PPh}_3)_3$, primarily the chlorido complex, which is the best behaved of the three. Aresta et al. noted in their original work that $\text{CoCl}(\text{PPh}_3)_3$ reacted with alkyl halides (RX) to give the coupled alkane product (R–R) along with free PPh_3 and $\text{CoCl}_2(\text{PPh}_3)_2$,⁸ indicating that the Co(I) complex could be involved in radical reactions, as is the case for cobalamins. In the late 1970s, the Cl and Br complexes were used for alkene dimerization reactions.^{23,24} In 1981, Yamada and Momose reported the use of $\text{CoCl}(\text{PPh}_3)_3$ for the reductive coupling of benzylic halides,²⁵ which is more useful for organic synthesis. Then, within the past few years, leading organic synthesis groups have made use of this compound as a stoichiometric reducing agent for the radical dimerization of halogenated organic molecules.^{26–28} $\text{CoCl}(\text{PPh}_3)_3$ succeeds in effecting reactions where other organic or inorganic reagents fail.^{26–28} Our goal is not specifically to develop better reagents for organic synthesis, but we believe that an understanding of the electronic structure of Co(I) in these systems can have practical applications as well as enhance our understanding of fundamental coordination chemistry.

EXPERIMENTAL SECTION

Synthesis. All operations were performed under nitrogen using Schlenk techniques or an MBraun LabMaster glovebox. Metal salts and triphenylphosphine were obtained from commercial sources; PPh_3 was recrystallized from toluene prior to use. Chlorido-tris(triphenylphosphine)cobalt(I), $\text{CoCl}(\text{PPh}_3)_3$, is commercially available from Sigma-Aldrich (catalog 361 844); however, as received, the material is bright blue rather than green. The blue color is indicative of (pseudo) tetrahedrally coordinated Co(II), such as found in $\text{CoCl}_2(\text{PPh}_3)_2$,²⁰ which, incidentally, is also available from Sigma-Aldrich. We had no interest in determining the exact nature of the commercial product, and instead prepared both $\text{CoCl}(\text{PPh}_3)_3$ and $\text{CoBr}(\text{PPh}_3)_3$ following the procedure of Aresta et al.⁸ In this procedure, $\text{CoX}_2 \cdot 6\text{H}_2\text{O}$ (X = Cl, Br) is reacted with 3 equiv of PPh_3 to generate a blue (for X = Cl) ethanolic solution of Co(II) phosphine halide species, which are then reduced by NaBH_4 to the desired product: a brown-green material for X = Cl and a green material for X = Br,

as reported by Aresta et al.⁸ These workers also used powdered Zn as a reductant; however, we found this to make the workup much more difficult and recommend use of only NaBH_4 . They also reported an analogous iodido complex, $\text{CoI}(\text{PPh}_3)_3$, but we were unable to reproduce their work and obtained only the Co(II) product, $\text{CoI}_2(\text{PPh}_3)_2$, which had been previously reported by others.²⁹ Aresta et al. had reported that the iodido complex is the least stable of the X series.⁸

UV–Vis–NIR. A Jasco V-570 spectrophotometer with a diffuse reflectance accessory was used to record spectra of solid $\text{CoCl}(\text{PPh}_3)_3$ and $\text{CoBr}(\text{PPh}_3)_3$ each diluted with MgO under a nitrogen atmosphere. Because the HFEPR studies were on solid material and solutions of $\text{CoX}(\text{PPh}_3)_3$ are extremely air sensitive, we focused mainly on solid state reflectance UV–vis–NIR spectra. Aresta et al. reported that the vis–NIR spectrum of $\text{CoCl}(\text{PPh}_3)_3$ in benzene solution in the presence of excess PPh_3 was the same as for the solid complex.⁸ In our hands, toluene solution spectra of $\text{CoCl}(\text{PPh}_3)_3$ with excess PPh_3 showed the expected vis–NIR bands, but also bands at ~ 600 nm characteristic of tetrahedral Co(II).^{30,31} We did find that solid state and toluene solution (with excess PPh_3) spectra of $\text{CoBr}(\text{PPh}_3)_3$ were qualitatively similar.

HFEPR. HFEPR spectra were recorded at NHMFL (Tallahassee, FL) using a spectrometer that differed from that described earlier³² only in the use of a Virginia Diodes (Charlottesville, VA) source operating at a base frequency of 12–14 GHz and multiplied by a cascade of multipliers. Some results originated from the Dresden High-Field Laboratory (HLD) using a similar setup.

Individual spectra were simulated using a standard spin Hamiltonian for $S = 1$:³³

$$\mathcal{H} = \beta_e B \cdot g \cdot \hat{S} + D[\hat{S}_z^2 - S(S+1)/3] + E[\hat{S}_x^2 - \hat{S}_y^2] \quad (1)$$

Computer fits were made to two-dimensional field versus frequency data sets to provide consensus frequency-independent spin Hamiltonian parameters. Further details of tunable-frequency HFEPR methodology are given elsewhere.¹⁸

LFT. Analysis of the electronic structure of Co(I) in the $\text{CoX}(\text{PPh}_3)_3$ series was performed with use of two approaches: crystal-field parametrization as described by Ballhausen,³⁴ and the angular overlap model (AOM), originally due to Schäffer.^{35,36} Two computer programs were employed, Ligfield, written by J. Bendix (Ørsted Institute, Copenhagen, Denmark),³⁷ and a locally written program, DDN, available from J. Telser. Both programs use the complete d^8 weak-field basis set including interelectronic repulsion (Racah parameters: B and C) and spin–orbit coupling (SOC) and either crystal-field (for DDN, the parameters: Dq , Ds , Dt)³⁴ or AOM ligand-field bonding parameters ($\varepsilon_{\sigma,\pi}$).³⁶ The two programs gave identical results when directly compared. The Ligfield program allows identification of the orbital occupancy and spin progeny of a given energy level (eigenstate). Representative Ligfield output files are given in Supporting Information. A version of the DDN program, DDNFIT, allows best fitting of the experimental electronic absorption band positions to values calculated by iteration of Racah and either crystal-field or AOM bonding parameters. Another version of the DDN program, DDNSUSFIT, allowed calculation of magnetic susceptibility data ($\chi_{\text{mol,para}}$, μ_{eff}) at various temperatures and applied fields.

For d block free-ions, definitive values for Racah parameters are given by Borson and Schäffer³⁸ and for SOC constants by Bendix, Borson, and Schäffer.³⁷ The free-ion parameters (in cm^{-1}) for Co(I) are $B = 798$, $C = 4382$ ($C/B = 5.49$, which value is unusually high),³⁸ and $\zeta = 466$.³⁷

QCT. All quantum chemical computations employed the software package ORCA (version 2.8.02), written by Neese and co-workers.³⁹ Two theoretical methods were employed: density functional theory (DFT) and unrestricted Hartree–Fock (UHF) theory. The ORCA calculations utilized the Ahlrichs type basis set VDZ⁴⁰ for H–Kr and auxiliary basis sets from the TurboMole library (ftp.chemie.uni-karlsruhe.de/pub/jbasen), as defined elsewhere,^{41–43} and the def2-TZV basis set.⁴⁴ Two representative, complete ORCA input/output files (for $\text{CoX}(\text{PR}_3)_3$, X = Cl, R = Ph, and X = Br, R = Me are given in

Supporting Information, along with the output portions of several other such files.

RESULTS AND DISCUSSION

Synthesis. We note that one of the papers describing the use of $\text{CoCl}(\text{PPh}_3)_3$ for organic synthesis mentioned that freshly prepared material was used.²⁸ Although we have no expertise in this application, we concur in that $\text{CoX}(\text{PPh}_3)_3$ compounds are exceedingly air sensitive and can decay over time to $\text{Co}(\text{II})$ products, which is presumably the fate of the commercially available material by the time it is received. However, the original report by Aresta et al. states that $\text{CoCl}(\text{PPh}_3)_3$ “is fairly stable to the air in the solid state, but not in solution”.⁸ We agree with this statement with respect to solution behavior. In typical organic solvents (toluene, dichloromethane), this reaction, which we believe to be relatively quantitative oxidation to $\text{Co}(\text{II})$ phosphine halides, is almost immediate (see Figure S1, Supporting Information). In our hands, however, these compounds even as solids are rather air unstable, oxidizing to blue $\text{Co}(\text{II})$ products in the course of a few minutes, and over days in closed screw-cap vials (see Figure S2, Supporting Information). Nevertheless, storage of freshly prepared material in sealed tubes and loading of HFEPR sample holders under Ar allowed recording of spectra free of $\text{Co}(\text{II})$ contaminants (see below).

Structures. The structure of $\text{CoCl}(\text{PPh}_3)_3$ exhibits 3-fold crystallographic symmetry (trigonal space group $P3$),⁹ as does that of $\text{CoCl}(\text{PMe}_3)_3$ (cubic space group $P\bar{a}3$).^{11,12} The structure of $\text{CoCl}(\text{PPh}_3)_3$ is shown in Figure 1. No structures

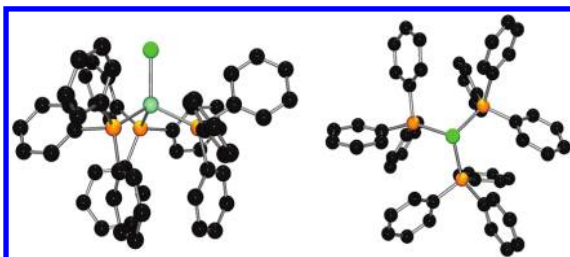


Figure 1. Structure of molecule 1 of $\text{CoCl}(\text{PPh}_3)_3$, as reported by Cassidy and Whitmire.⁹ At left is a view normal to the $\text{Co}-\text{Cl}$ bond (C_3 axis); at right is a view down the C_3 axis. The color scheme is as follows: Co, aquamarine; Cl, green; P, orange; C, black.

have been reported for $\text{CoBr}(\text{PR}_3)_3$ ($\text{R} = \text{Me, Ph}$) or $\text{CoI}(\text{PPh}_3)_3$; however, the structure of $\text{CoI}(\text{PMe}_3)_3$ is only 2-fold symmetric (monoclinic space group $P2_1/m$).¹³ The air sensitivity of $\text{CoBr}(\text{PPh}_3)_3$ in solution has prevented us from growing crystals of this complex; however, as shown below, HFEPR indicates that it also has 3-fold symmetry. Metric parameters related to the coordination sphere of $\text{Co}(\text{I})$ in these $\text{CoX}(\text{PR}_3)_3$ complexes are given in Table S1 (Supporting Information), which includes the two complexes with chelating ligands. The difference in these parameters between the chlorido triphenylphosphine and trimethylphosphine complexes is essentially the same as the difference among different molecules of a given complex whether in the same unit cell or in different structure determinations. Even the iodido complex is very similar to the chlorido structures, except for the longer $\text{Co}-\text{I}$ bond. The parameters for the bromido complex, $\text{CoBr}(\text{NP}3)$, are also quite similar to those for the chlorido complexes, despite the tridentate chelating nature of the ligand. This suggests that the absence of a crystal structure for

$\text{CoBr}(\text{PPh}_3)_3$ is not critical. Only the triphos complex shows a significant difference from the others due to the demands of this tridentate ligand.

UV–Vis–NIR. In contrast to the bright blue color typical of tetrahedral $\text{Co}(\text{II})$ complexes, the $\text{Co}(\text{I})$ complexes are green in the solid state and in noncoordinating solvents (toluene, dichloromethane). Because the HFEPR studies were conducted on solids, and in view of the extreme solution sensitivity of these complexes (see Figure S1), we only qualitatively confirmed the result of Aresta et al.⁸ that $\text{CoX}(\text{PPh}_3)_3$ compounds have the same electronic absorption spectra in solution (they used benzene with excess PPh_3 ; we used toluene with excess PPh_3) as in the solid state. The results are summarized in Table 1, and reflectance spectra are shown in Figure 2, which also shows a toluene solution spectrum for the bromido complex. This complex appeared to be more stable in solution than the chlorido complex.

HFEPR. Both $\text{CoCl}(\text{PPh}_3)_3$ and $\text{CoBr}(\text{PPh}_3)_3$ examined as polycrystalline solids showed a strong EPR response at frequencies above 90 GHz and at liquid helium temperatures. Upon warming the samples, the intensity of the resonances decreased, but they were still easily detectable even at room temperature (295 K). No signals were observed near $g \approx 2.0$ in $\text{CoCl}(\text{PPh}_3)_3$ and only weak resonances in $\text{CoBr}(\text{PPh}_3)_3$ at $g \approx 2.05–2.15$, indicating the absence of other than impurity-level organic radical or metal-centered paramagnet, which could arise from species such as $\text{Co}(0)$ ($3d^9, S = 1/2$) or, more likely, low spin (LS) $\text{Co}(\text{II})$ or high-symmetry high-spin (HS) $\text{Co}(\text{II})$. More importantly, no signals were seen anywhere in the field range that could be attributed to lower-symmetry HS $\text{Co}(\text{II})$, such as we have observed for $\text{CoX}_2(\text{PPh}_3)_2$, $\text{X} = \text{Cl, Br, I}$.

Figures 3 and 4 show representative HFEPR spectra for $\text{CoCl}(\text{PPh}_3)_3$ and $\text{CoBr}(\text{PPh}_3)_3$, respectively, in the high frequency and low temperature regime. In both cases, the spectra were found to be a combination of three distinct triplet ($S = 1$) states, labeled A, B, C in the order of increasing zfs parameters, and could be well simulated as a sum of these three components. The intensities of the EPR signals corresponding to sites A and B are approximately equal, as can be seen by eye in Figures 3 and 4. While the amplitude of triplet C is lower by a factor of ca. 3.5 than those of A and B, after taking into account an increase of line width by a factor of 2 (for the best-defined perpendicular $\Delta M_S = \pm 1$ turning points) its integrated intensity is about the same as those of species A and B; i.e., the ratio of the three species is approximately 1:1:1.

Although the agreement between experiment and simulation in Figures 3 and 4 can be deemed very good, the actual simulation parameters were obtained not from single-frequency spectra such as those in the two figures, but from two-dimensional field/frequency maps obtained for each of the two complexes along the principle of tunable-frequency EPR.¹⁸ Figures 5 and 6 show such maps consisting of experimental resonances represented by symbols, and simulations represented by curves, for each of the three triplet states found for each molecule. Simulation parameters were obtained by a least-squares fit to the complete data set for each of the triplets as explained elsewhere¹⁸ and are shown in Table 2.

A striking feature of each of the triplets in both complexes is the strict axiality of their zfs tensors. No splitting of the perpendicular turning points into x and y components could be observed. HFEPR is able to detect very small deviations from axial symmetry, in both relative and absolute terms. In this case, simulations indicate a maximum rhombicity, $|E/D|$, of at most

Table 1. Electronic Absorption Spectra of $\text{CoX}(\text{PPh}_3)_3$ Complexes

	Assignment ^a			
cubic	$^3\text{T}_1(\text{P}) \leftarrow ^3\text{T}_1(\text{F})$		$^3\text{A}_2(\text{F}) \leftarrow ^3\text{T}_1(\text{F})$	$^3\text{T}_2(\text{F}) \leftarrow ^3\text{T}_1(\text{F})$
trigonal A_2	$^3\text{E}(\text{P}) \leftarrow ^3\text{A}_2$	$^3\text{A}_2(\text{P}) \leftarrow ^3\text{A}_2$	$^3\text{A}_2(\text{F}) \leftarrow ^3\text{A}_2$	$^3\text{A}_1, ^3\text{E} \leftarrow ^3\text{A}_2$
trigonal E	$^3\text{A}_2(\text{P}) \leftarrow ^3\text{E}$	$^3\text{E}(\text{P}) \leftarrow ^3\text{E}$	$^3\text{A}_2(\text{F}) \leftarrow ^3\text{E}$	$^3\text{A}_1, ^3\text{E} \leftarrow ^3\text{E}$
		CoCl(PPh_3) ₃		
toluene soln ^b	13 430 (745)	10 400 (960, sh)	9350 (1070)	
diff reflect ^b	13 700 (730)	10 400 (960, sh)	9090 (1100)	5100 (1960)
Aresta et al. ^c	13 420 (745)	10 650 (940, sh)	9090 (1100)	5000 (2000)
		Calcd ^d		
cubic	13 400		9400	4350
trigonal A_2	12 840	11 560	8940	4200, 4950
trigonal E	13 380	10 540	9480	5710, 4360
AOM $\sigma, \pi \text{ A}_2^e$	13 420 ^f	10 650 ^f	9090	5260, 5000
AOM $\sigma \text{ E}^e$	13 040	11 690	9300	4950, 4220
		CoBr(PPh_3) ₃		
toluene soln ^b	13 350 (750)	10 300 (970, sh)	9270 (1080)	
diff reflect ^b	13 500 (740)	10 350 (965, sh)	9050 (1105)	4750 (2100)
Aresta et al. ^c	13 250 (755)	10 520 (950, sh)	8970 (1115)	4650 (2150)
		Calcd ^d		
cubic	13 250		9210	4260
trigonal A_2	12 650	11 390	8780	4060, 4750
trigonal E	13 220	10 470	9220	5520, 4220
		CoI(PPh_3) ₃		
Aresta et al. ^c	12 580 (795)		8620 (1160)	4540 (2200)
		Calcd ^d		
cubic	12 590		8840	4090

^aExperimental band positions in cm^{-1} and nm (in parentheses); calculated values in cm^{-1} . The upper row corresponds to the transition in T_d point group symmetry. The lower row corresponds to the transition in C_{3v} point group symmetry; in this case, two choices are possible for the ground state (since T_1 splits into A_2 and E), as indicated. ^bThis work. Toluene solution (with excess PPh_3) and diffuse reflectance spectra. The bands are broad, and the uncertainty in maxima is ± 5 nm for $\lambda < 1100$ nm and ± 50 nm ($\sim 50 \text{ cm}^{-1}$) for $\lambda > 1100$ nm. No attempt was made to record solution spectra at $\lambda > 1100$ nm. ^cReference 8. Benzene solution (with excess PPh_3) spectra. The molar absorptivity of these bands in the chlorido and bromido complexes was in the range $100\text{--}150 \text{ M}^{-1} \text{ cm}^{-1}$, typical for d-d transitions; no values were reported for the iodido complex. ^dValues are rounded to the nearest 10 cm^{-1} . The topmost row corresponds to a calculation using only cubic (T_d) crystal field splitting and ignoring the shoulder seen for the Cl and Br complexes. Parameters (all in cm^{-1}) used for Cl: $B = 650$, $Dq = 505$. For Br: $B = 645$, $Dq = 495$. For I: $B = 610$, $Dq = 475$. The second and third rows correspond to calculations using trigonal crystal field splitting as well and including the shoulder band. Transition energies to both $^3\text{A}_1$ and ^3E excited states originating from $^3\text{T}_2$ are calculated; however, only transitions to ^3E are fitted. In the second row, $Ds < 0$, which gives a $^3\text{A}_2[^3\text{T}_1(\text{F})]$ ground state. In the third row, $Ds > 0$, which gives a $^3\text{E}[^3\text{T}_1(\text{F})]$ ground state. Parameters (all in cm^{-1}) used for Cl, $^3\text{A}_2$: $B = 525$, $Dq = 480$, $Ds = -580$. For Cl, ^3E : $B = 445$, $Dq = 510$, $Ds = +760$. For Br, $^3\text{A}_2$: $B = 530$, $Dq = 470$, $Ds = -525$. For Br, ^3E : $B = 450$, $Dq = 495$, $Ds = +740$. No such calculation was done for the iodido complex. ^eThese two rows correspond to AOM calculations using the structural data for molecule 1 of $\text{CoCl}(\text{PPh}_3)_3$ (see Table S1). The upper of these two rows (fourth overall) includes both σ and cylindrical π -bonding, with the phosphines as acceptors and the chloride as a donor, with the following parameters: $B = 450$, $\varepsilon_{\sigma}(\text{P}) = 3340$, $\varepsilon_{\pi}(\text{P}) = -310$, $\varepsilon_{\sigma}(\text{Cl}) = 5430$, $\varepsilon_{\pi}(\text{Cl}) = +1380$, which gives a $^3\text{A}_2$ ground state. The lower of these two rows (fifth overall) corresponds to a calculation using only σ -bonding, with the following parameters: $B = 545$, $\varepsilon_{\sigma}(\text{P}) = 3250$, $\varepsilon_{\sigma}(\text{Cl}) = 5190$, which gives a ^3E ground state. No such calculations were done for the bromido or iodido complexes because no structures have been determined. ^fUsing this model, the transition at lower energy is actually $^3\text{E}(\text{P}) \leftarrow ^3\text{A}_2$, and that at higher energy is $^3\text{A}_2(\text{P}) \leftarrow ^3\text{A}_2$, the same ordering as for the trigonal crystal-field model with a ^3E ground state; however, these entries are transposed so that the energy match is clear.

0.002. This rigorous axiality is consistent with the crystallographic symmetry, as described above. Correspondingly, the g tensors are also axial, and close to isotropic, with the range of g values contained between 2.20 and 2.25 for g_{\perp} and 2.16 and 2.25 for g_{\parallel} . The axial zfs parameter D varies from about 4–8 cm^{-1} for $\text{CoCl}(\text{PPh}_3)_3$ to about 2–7 cm^{-1} for $\text{CoBr}(\text{PPh}_3)_3$. In each case D is positive, as found by simulations of single-frequency spectra. The single-crystal line width used in simulations is approximately the same (50 mT) for triplets A and B in both complexes, while triplet C, characterized by the largest D, has also much larger line width of about 100 mT (all the values given are for the allowed, $\Delta M_S = \pm 1$ transitions.)

LFT Analysis. The initial analysis will use a crystal field model that includes only cubic splitting (given by the Ballhausen parameter, Dq ³⁴) and interelectronic repulsion,

given by the Racah parameter B (only triplet states will be considered at this point, so the Racah parameter C is not relevant).³⁶ This method has recently been used to analyze electronic absorption spectra of pseudotetrahedral Ni(II) alkoxide complexes.⁴⁵ The results are given in Table 1 and include $\text{CoI}(\text{PPh}_3)_3$ even though this complex was not studied here. The fit is not perfect, which is hardly surprising given the crude nature of the model, but the transition $^3\text{T}_1(\text{P}) \leftarrow ^3\text{T}_1(\text{F})$ can be matched exactly and the other two ($^3\text{T}_2 \leftarrow ^3\text{T}_1(\text{F})$ and $^3\text{A}_2 \leftarrow ^3\text{T}_1(\text{F})$) are within 300–500 cm^{-1} ; the experimental precision of the last of these bands (well into the NIR region) is relatively low. The fit parameters (in cm^{-1}) are all relatively close: $610 \leq B \leq 650$ and $475 \leq Dq \leq 505$, in the order I < Br < Cl, which is consistent with the spectrochemical series. That the crystal field parameters for the three different halido

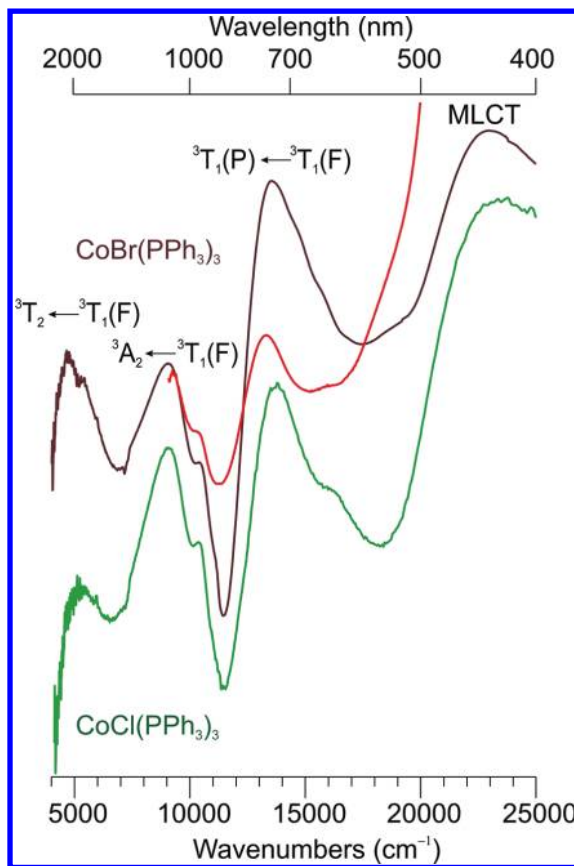


Figure 2. Diffuse reflectance spectra of $\text{CoCl}(\text{PPh}_3)_3$ (green trace) and $\text{CoBr}(\text{PPh}_3)_3$ (brown trace). The red trace shows the electronic absorption spectrum of $\text{CoBr}(\text{PPh}_3)_3$ in toluene solution (ca. 4 mM) in the presence of excess PPh_3 . The ordinate is in arbitrary units. The assignment of bands is for idealized tetrahedral symmetry.

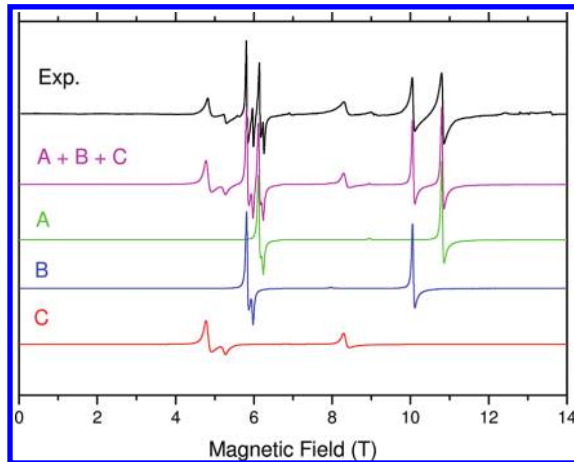


Figure 3. HFEPR spectra of polycrystalline $\text{CoCl}(\text{PPh}_3)_3$ at 406.4 GHz, and 10 K. The black trace is an experimental result, while the colored traces represent simulations for the three individual triplet states identified in the sample (green = A, blue = B, red = C), and also their sum (magenta trace). Simulation parameters are those from Table 3. Single crystal line widths: for triplets A and B, 50 mT isotropic for the $\Delta M_S = \pm 1$ transitions, 20 mT for the $\Delta M_S = \pm 2$ transition; for triplet C, 100 mT isotropic for the $\Delta M_S = \pm 1$ transitions, 20 mT for the $\Delta M_S = \pm 2$ transition.

complexes are so close is presumably the consequence of the constancy of the three phosphino ligands. Given that free-ion

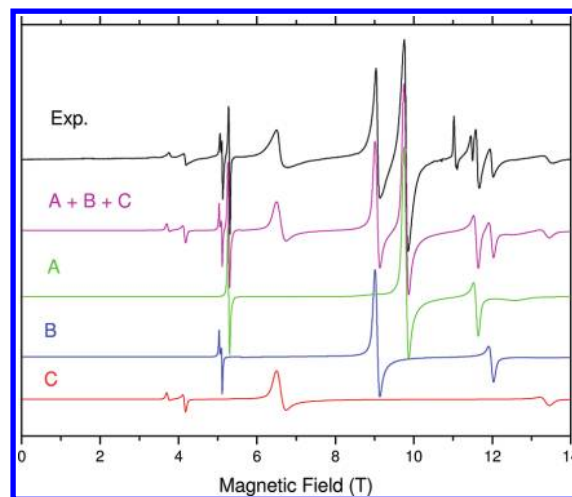


Figure 4. HFEPR spectra of polycrystalline $\text{CoBr}(\text{PPh}_3)_3$ at 331.2 GHz, and 10 K. The black trace is an experimental result, while the colored traces represent simulations for the three individual triplet states identified in the sample (green = A, blue = B, red = C), and also their sum (magenta trace). Simulation parameters are those from Table 3. Single crystal line widths were the following: triplet A, 50/250 mT for the perpendicular/parallel turning points, respectively, in $\Delta M_S = \pm 1$ transitions, 20 mT for the $\Delta M_S = \pm 2$ transition; triplet B, 50/250 mT for the perpendicular/parallel turning points, respectively, in $\Delta M_S = \pm 1$ transitions, 10 mT for the $\Delta M_S = \pm 2$ transition; triplet C, 100 mT isotropic for the $\Delta M_S = \pm 1$ transitions, 20 mT for the $\Delta M_S = \pm 2$ transition. The two resonances observed near 11.05, and 11 T ($g = 2.15$, and 2.05, respectively), are due to impurities not belonging to the triplet states characteristic for the bulk complex, and are not simulated.

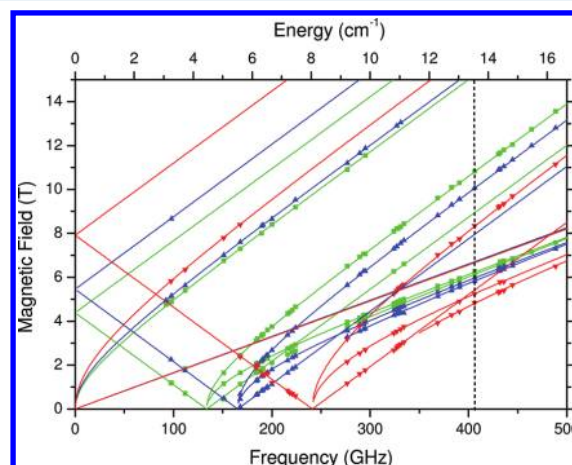


Figure 5. Field/frequency map of resonances observed in $\text{CoCl}(\text{PPh}_3)_3$ at 10 K. Symbols (■, ▲, ▼) are experimental points; curves were simulated using spin Hamiltonian parameters from Table 2. Different colors denote the three different triplet states identified in this complex (green = triplet A, blue = B, red = C). The vertical dashed line represents the frequency at which the spectrum in Figure 3 was recorded.

$\text{Co}(\text{I})$ has $B = 798 \text{ cm}^{-1}$,³⁸ we find that $75\% < B/B_{\text{free-ion}} < 80\%$, which is reasonable for a covalent complex.³⁶

This crystal-field model can be extended to describe the trigonal distortion introduced by the symmetry of the molecule, which causes ${}^3\text{T}_1(\text{F},\text{P})$ to split into ${}^3\text{A}_2$ and ${}^3\text{E}$, and ${}^3\text{T}_2$ to split into ${}^3\text{A}_1$ and ${}^3\text{E}$. The ground state could be either ${}^3\text{E}[{}^3\text{T}_1(\text{F})]$ or ${}^3\text{A}_2[{}^3\text{T}_1(\text{F})]$ and almost all possible transitions are allowed in C_{3v} symmetry: $\text{A}_2 \leftrightarrow \text{A}_2$ with z polarization, and $\text{E} \leftrightarrow \text{A}_1$, $\text{E} \leftrightarrow \text{A}_2$,

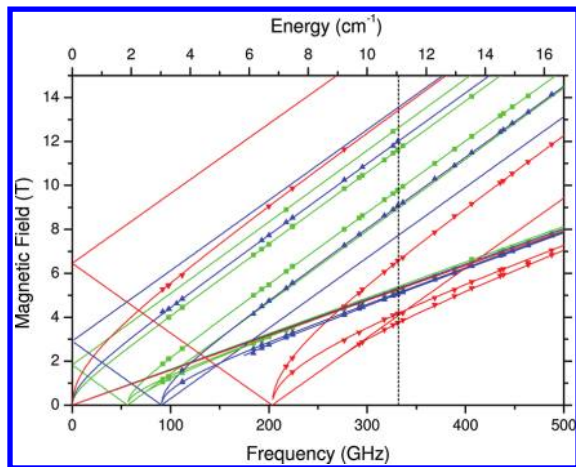


Figure 6. Field/frequency map of resonances observed in $\text{CoBr}(\text{PPh}_3)_3$ at 10 K. Symbols (\blacksquare , \blacktriangle , \blacktriangledown) are experimental points; curves were simulated using spin Hamiltonian parameters from Table 2. Different colors denote the three different triplet states identified in this complex (green = triplet A, blue = B, red = C). The vertical dashed line represents the frequency at which the spectrum in Figure 4 was recorded.

and $E \leftrightarrow E$ all with xy polarization; only $A_1 \leftrightarrow A_2$ is symmetry forbidden. Unfortunately, we have no polarization data, and the vis–NIR spectra of $\text{CoX}(\text{PPh}_3)_3$ are insufficiently resolved to allow assignment of this trigonal splitting; it is only hinted at by the shoulder seen at $10\,500\text{ cm}^{-1}$ in the chlorido and bromido complexes (see Table 1). There are two possible assignments: either this shoulder is assigned to the transition ${}^3\text{E}[{}^3\text{T}_1(\text{P})] \leftarrow {}^3\text{E}[{}^3\text{T}_1(\text{F})]$ or to ${}^3\text{A}_2[{}^3\text{T}_1(\text{P})] \leftarrow {}^3\text{A}_2[{}^3\text{T}_1(\text{F})]$ (fitting with this model shows that the ${}^3\text{T}_1(\text{F})$ ground state splits in the same order as the ${}^3\text{T}_1(\text{P})$ excited state). We have no reliable information on splitting of the ${}^3\text{T}_2$ state; however, fitting is helpfully constrained by ignoring the transition to ${}^3\text{A}_1[{}^3\text{T}_2]$ since ${}^3\text{A}_1[{}^3\text{T}_2] \leftarrow {}^3\text{A}_2[{}^3\text{T}_1(\text{F})]$ is forbidden. The trigonal splitting is parametrized by D_s . For $D_s > 0$, the ground state is ${}^3\text{E}[{}^3\text{T}_1(\text{F})]$ and the transitions for both the chlorido and bromido complexes are well fitted with little change in Dq from the cubic only fit (still $\sim 500\text{ cm}^{-1}$), although with a significant reduction in B (from ~ 650 to $\sim 450\text{ cm}^{-1}$; see Table 1). For $D_s < 0$, the ground state is ${}^3\text{A}_2[{}^3\text{T}_1(\text{F})]$ and the transitions for both the chlorido and bromido complexes are again well fitted, although not quite as well as with the ${}^3\text{E}$ ground state, likewise with little change in Dq , but a lesser reduction in B (to $\sim 530\text{ cm}^{-1}$; see Table 1). On the basis of this analysis of the electronic absorption spectrum alone, there is no way to distinguish unequivocally between these two ground states. The fit value of B relative to the free-ion value for the orbital doublet ground state is lower than what might be considered appropriate ($\sim 50\%$), but this is no basis for excluding this possibility.

With this reasonably successful model for the electronic absorption spectra at hand, we can proceed to include spin–orbit coupling and see if the zfs observed by HFEPR can be reproduced. In this case, a serious problem results, but of a different nature than that seen in our other applications of LFT, which tend to underestimate zfs. Use of $\zeta = 230\text{ cm}^{-1}$, 50% of the free-ion value, gives a positive D value ($M_S = 0$ spin ground state), but with a magnitude that is far above what is seen experimentally, 32 cm^{-1} versus $5\text{--}8\text{ cm}^{-1}$, respectively. In order to reduce the zfs into this experimental range, a range of

Table 2. Experimental Axial $S = 1$ Spin Hamiltonian Parameters for $\text{CoX}(\text{PPh}_3)_3$, $\text{X} = \text{Cl}, \text{Br}$, from HFEPR Measurements and Magnetic Susceptibility Data, with Calculations (in Brackets)

complex, species ^a	D (cm^{-1}) ^b	g_{\perp}	g_{\parallel}	μ_{eff}^c 77 K, 294 K
$\text{CoCl}(\text{PPh}_3)_3$				
triplet A	+4.46(1)	2.200(3)	2.178(5)	
molecule 2	[+4.71]	[2.251]	[2.065]	[3.057, 3.076]
triplet B	+5.512(3)	2.222(1)	2.164(4)	
molecule 3	[+5.66]	[2.275]	[2.064]	[2.997, 3.094]
triplet C	+8.04(1)	2.225(2)	2.18(1)	
molecule 1	[+8.07]	[2.362]	[2.050]	[3.009, 3.155]
av ^c	+6.00			3.04, 3.11
trigonal A_2	[+5.97]			[3.010, 3.098]
AOM $\sigma, \pi A_2$	[+6.15]			[3.021, 3.108]
$\text{CoBr}(\text{PPh}_3)_3$				
triplet A	+1.873(6)	2.204(1)	2.195(3)	
triplet B	+3.03(1)	2.227(1)	2.227 ^d	
triplet C	+6.78(1)	2.243(2)	2.25(2)	
av ^c	+3.89			3.08, 3.17

^aThree distinct $S = 1$ species with axial symmetry were observed for each sample and are denoted triplets A, B, C. These can be related by LFT to the three molecules observed crystallographically for $\text{CoCl}(\text{PPh}_3)_3$ as indicated here (see text for details). The AOM bonding parameters used for the LFT calculation of spin Hamiltonian parameters of each molecule are given in Table 4, combined with $\zeta = 101\text{ cm}^{-1}$ (chosen to match the D value for molecule 1, i.e., the largest zfs) and Racah $B = 450$, $C = 2470\text{ cm}^{-1}$ ($C = 5.49B$, as in the free ion³⁸). Magnetic susceptibility calculations use in addition the electronic Zeeman interaction, $\mathcal{H}_Z = \beta H \cdot (kL + g_e S)$ with $k = 0.52$ and $H = 1\text{ kOe}$; values calculated using $H = 100\text{ kOe}$ differed by only $\sim 0.02\%$ from the lower field calculation. Magnetic susceptibility was also calculated using the trigonal crystal-field model with an ${}^3\text{A}_2$ ground state (the more viable model; see text) and the parameters given in Table 2, combined with $\zeta = 108\text{ cm}^{-1}$ (chosen to match the average D value) and Racah $B = 525$, $C = 2880\text{ cm}^{-1}$. ^bValues only for D (axial component of zfs) are given. Simulations allow an estimate as to the maximum value for E (rhombic component of zfs) as follows: triplets A and B, 0.010 cm^{-1} ; triplet C, 0.015 cm^{-1} . These values correspond to a maximum rhombicity of $|E/D| \approx 0.002$ for all three triplets. ^cPowder magnetic susceptibility data, taken from Aresta et al.,⁸ provides only an average of the three species seen crystallographically and by HFEPR. Averages for both experimental and calculated D values are provided for convenience only; no such value is observed experimentally. ^dHere the g_{\parallel} value was assumed to be equal to g_{\perp} ; no parallel turning points observed.

$100\text{ cm}^{-1} \leq \zeta \leq 130\text{ cm}^{-1}$ is needed, $\sim 25\%$ of the free-ion value.⁴⁶ What about the ${}^3\text{E}$ ground state (from $D_s > 0$)? In this case, a spin Hamiltonian is totally unsuccessful in describing how this state is transformed under spin–orbit coupling. Regardless of the magnitude of ζ , the ground state is a nonmagnetic singlet, and thus would give rise to no HFEPR; the lowest excited state is the same (at $\sim \zeta/4$ above the ground state), and there is then a magnetic doublet, but with $M_S \approx 0$ (at $\sim \zeta/2$), and last a magnetic doublet with $M_S \approx \pm 1$ (at $\sim \zeta$). Therefore, only by assuming that the ground state is the orbital singlet, ${}^3\text{A}_2[{}^3\text{T}_1(\text{F})]$, can the experimental HFEPR results be even remotely modeled (despite the magnitude of D being overestimated, albeit with correct sign).

Alternatively to the crystal field method, the angular overlap model (AOM) can be used to analyze the electronic structure of the structurally characterized complex, $\text{CoCl}(\text{PPh}_3)_3$, as has

been done for analogous four-coordinate complexes of Ni(II).^{21,47,48} The crystallographic 3-fold symmetry of $\text{CoCl}(\text{PPh}_3)_3$ means that each of the three independent molecules in the unit cell has only one metric parameter for the AOM: the angle θ , defined by the Cl–Co–P bond angle, which is distorted by $+4.2^\circ$ from ideal T_d symmetry (see Table S1; the ϕ angles are exactly $2\pi n/3$, $n = 0, 1, 2$). The question then is, what values to use for the AOM bonding parameters $\varepsilon_{\sigma,\pi}$ (P1, Cl1)? Both PPh_3 and the halido ligands are cylindrical in their π -bonding,^{49,50} so there is only one ε_π value for each ligand type, with $\varepsilon_\pi(\text{P1}) \leq 0$ (π -acceptor) and $\varepsilon_\pi(\text{Cl1}) \geq 0$ (π -donor). Initial estimates as to these values can be made based on previous studies of Co(II) and Ni(II) phosphino/halido complexes.^{21,49–51} We can also use the estimate of Dq made above by noting that

$$Dq = \frac{2}{15} \left(\varepsilon_\sigma - \frac{4}{3} \varepsilon_\pi \right)$$

where Dq is taken as positive, although strictly speaking it is negative for tetrahedral complexes. If we neglect π -bonding, then $\varepsilon_\sigma \approx 3750 \text{ cm}^{-1}$, which is low relative to the previously studied systems; however, the charge on the metal ion is lower here.

We can then attempt to fit the observed electronic transitions using the AOM first with only σ -bonding, using assignments as above with the crystal-field model. With only σ -bonding (i.e., three variables), it is possible to fit the electronic transitions quite well (see Table 1); however, the resulting ground state is ${}^3\text{E}[{}^3\text{T}_1(\text{F})]$, which is unreasonable, as described above. In order to obtain the ${}^3\text{A}_2[{}^3\text{T}_1(\text{F})]$ ground state, π -bonding must be included.⁵² In this case, it is possible to fit the observed bands beyond the experimental precision (admittedly now with five variables), as shown in Table 1. Note that the ordering of the excited states with π -bonding is not quite the same as with the crystal field model; in particular the shoulder must be assigned to ${}^3\text{E}[{}^3\text{T}_1(\text{P})] \leftarrow {}^3\text{A}_2[{}^3\text{T}_1(\text{F})]$. The results show weak π -acceptance by the phosphine ligands and relatively strong π -donation by the chlorido ligand. The orbital description of the ground and excited states is determined by the Ligfield program, and the results for only the triplet states are given in Supporting Information. These show that the orbital ground state in this trigonal system can be described by $(\text{d}_z^2)^{2.00}(\text{d}_{xy,x^2-y^2})^{3.33}(\text{d}_{xz,yz})^{2.67}$ in the absence of SOC.

In Table 3, the AOM results are compared to those for $\text{NiCl}_2(\text{PPh}_3)_2$.²¹ Similar parameters were reported by Gerloch and Hanton for the PPh_3 ligand in $[\text{Ni}(\text{PPh}_3)\text{X}_3]^-$ ($\text{X} = \text{Br}, \text{I}$).⁵⁰ It would be of interest to study the complex that in some way links these two, namely $\text{NiCl}(\text{PPh}_3)_3$,⁹ for which the (conventional) EPR spectrum of this 3d⁹ complex (to our knowledge not reported) would also be helpful.

Nevertheless, the same problem obtains with the AOM as with the crystal field model when the zfs is calculated. The sign is correct, but the SOC must be small to keep the magnitude within range; $\zeta = 100 \text{ cm}^{-1}$ gives $D \approx 8 \text{ cm}^{-1}$ (see Ligfield output with SOC in Supporting Information). Another consideration is spin–spin coupling (SSC), which has been shown by Neese and co-workers to be significant not only in organic triplets,⁵³ but also in $S > \frac{1}{2}$ transition metal complexes.^{54,55} We have no ability to include this effect in our AOM, although it is determined in the QCT calculations described below and appears to be relatively small.

Table 3. AOM Parameters for 3d⁸ $\text{CoCl}(\text{PPh}_3)_3$ and $\text{NiCl}_2(\text{PPh}_3)_2$ (Values in cm^{-1})^a

complex	$\varepsilon_\sigma(\text{Cl})$	$\varepsilon_\pi(\text{Cl})$	$\varepsilon_\sigma(\text{P})$	$\varepsilon_\pi(\text{P})$
$\text{CoCl}(\text{PPh}_3)_3$ ^b				
molecule 1	5430	+1380	3340	-310
molecule 2	5310	+1350	3470	-322
molecule 3	5190	+1320	3435	-319
$\text{NiCl}_2(\text{PPh}_3)_2$ ^c	5300	+2400	5550	-1200

^aCylindrical π -bonding is assumed; all ligands of the same type are assumed to be equivalent. ^bThis work. Values based on crystal structure,⁹ electronic absorption data, and HFEPR indicating a ${}^3\text{A}_2$ ground state. ^cConsensus values from Krzystek et al.²¹ Both the electronic absorption data and HFEPR data were fitted.

A final consideration, which may well be the crucial one, is the contribution from spin delocalization onto the halido and phosphine ligands, which have non-negligible SOC constant values of their own.^{56–59} Atomic Cl, and especially Br and I due to their large SOC constants and lower electronegativity, are relevant due to the potential contribution to the formally $\text{Co(I)}\text{–halido}$ complex, $\{\text{Co}^+\text{–X}^-\}$, of what can be crudely represented as $\{\text{Co}^0\text{–X}^0\}$. In the case of the phosphine ligands, what could be represented as $\{\text{Co}^{2+}\text{–P}^-\}$ and/or $\{\text{Co}^0\text{–P}^+\}$ might even be contributing, noting that there are three of these P donors. SOC from these ligands could well be opposite in their contribution to zfs to that from the Co(I) ion, leading to near cancellation of zfs. Such effects have been seen for Mn(III) with iodido ligands (where a reversal of the sign of D from that expected was seen),⁶⁰ and for Ni(II) with a series of halido ligands, where the D value ranged from small magnitude and positive to large magnitude and negative as X changed from Cl to Br to I.^{47,61}

Despite these difficulties, it is instructive to use the AOM to attempt to take into account the slight variation in Co–Cl and Co–P bond lengths, as this is the only possible basis for the multiple species observed by HFEPR. Larrabee et al. assumed an r^{-5} dependence of σ -bonding strength on bond distance (r) in their studies of high-spin Co(II) systems,⁶² which they based on studies by Lever et al. on six-coordinate Ni(II) with amine N (i.e., pure σ donors).⁶³ We are uncertain as to how to handle the dependence on r of π -bonding, but initially, we use the Co–Cl and Co–P bond lengths in molecule 1 as the base (see Table S1) and assuming an r^{-5} dependence of both σ - and π -bonding, obtain the following relations: $\varepsilon_{\sigma,\pi}(\text{Cl}2) = 0.978 \times \varepsilon_{\sigma,\pi}(\text{Cl}1)$, $\varepsilon_{\sigma,\pi}(\text{Cl}3) = 0.956 \times \varepsilon_{\sigma,\pi}(\text{Cl}1)$, and $\varepsilon_{\sigma,\pi}(\text{P}2) = 1.039 \times \varepsilon_{\sigma,\pi}(\text{P}1)$, $\varepsilon_{\sigma,\pi}(\text{P}3) = 1.028 \times \varepsilon_{\sigma,\pi}(\text{P}1)$. The slight change in θ (see Table S1), for which there is a direct experimental basis, is also included. The resulting AOM parameters are given in Table 3. Use of $\zeta = 101 \text{ cm}^{-1}$ gives the following calculated D values (in cm^{-1}): +8.07 (molecule 1), +5.66 (molecule 3), +4.71 (molecule 2), comparable to the experimental values +8.04 (triplet C), +5.51 (triplet B), +4.46 (triplet A). These values are compiled in Table 2. The very good match may be fortuitous, but it does demonstrate that seemingly minor crystallographic differences can be reflected in zfs parameters that are readily detected by the high precision possible using HFEPR. Use of these three models also allows determination of g values by calculations with an external magnetic field, as described elsewhere. The results are given in Table 2, and although the match is not ideal (g_{\perp} is overestimated and g_{\parallel} is underestimated; as discussed elsewhere, LFT tends to give

Table 4. QCT Computational Results (using DFT and UHF) on $\text{CoX}(\text{PR}_3)_3$ ($\text{X} = \text{F}, \text{Cl}, \text{Br}, \text{I}; \text{R} = \text{Me}, \text{Ph}, \text{CH}_2-$): Calculated Spin Singlet – Triplet Difference Energies and Calculated zfs (All Energies in cm^{-1}) and g Value Matrices for Triplet State

complex	singlet – triplet		$D, E ^j$		g	
	DFT	UHF	DFT	UHF	DFT	UHF
$\text{CoCl}(\text{PPh}_3)_3^a$						
KOCVON molecule 1	12 549	<i>k</i>	+0.91, 0.02	+10.30, 0.02	[2.079, 2.082, 2.083]	[2.280, 2.390, 2.390]
KOCVON molecule 2	11 991	<i>k</i>	+1.16, 0.02	<i>m</i>	[2.072, 2.080, 2.081]	<i>m</i>
KOCVON molecule 3	12,190	<i>k</i>	+0.98, 0.01	+12.89, 0.01	[2.075, 2.082, 2.082]	[2.259, 2.398, 2.398]
$\text{CoF}(\text{PPh}_3)_3^b$ from KOCVON molecule 1 Co–F 2.07 Å			+0.08, 0.02	+20.79, 0.02	[2.072, 2.087, 2.088]	[2.216, 2.456, 2.457]
$\text{CoBr}(\text{PPh}_3)_3^c$ from KOCVON molecule 1 Co–Br 2.365 Å			+11.94, 0.009	+14.44, 0.02	[2.088, 2.088, 2.094]	[2.313, 2.394, 2.394]
$\text{CoI}(\text{PPh}_3)_3^d$ from KOCVON molecule 1 Co–I 2.549 Å			+42.31, 0.08	+30.28, 0.02	[2.098, 2.098, 2.116]	[2.362, 2.401, 2.401]
$\text{CoCl}(\text{PMe}_3)_3^e$						
BUTDEZ	11 665	<i>k</i>	+2.19, 0.00	+6.141, 0.227	[2.057, 2.063, 2.063]	[2.177, 2.271, 2.271]
BUTDEZ01	11 835	<i>k</i>	+2.20, 0.00	+10.25, 0.00	[2.053, 2.064, 2.064]	[2.164, 2.289, 2.289]
$\text{CoBr}(\text{PMe}_3)_3^f$ from BUTDEZ01						
Co–Br 2.365 Å	11 663	<i>k</i>	+14.48, 0.00	+5.802, 0.0	[2.065, 2.073, 2.073]	[2.184, 2.298, 2.298]
Co–Br 2.375 Å	11 916	<i>k</i>	+14.25, 0.00	+5.850, 0	[2.065, 2.074, 2.074]	[2.184, 2.299, 2.299]
$\text{CoI}(\text{PMe}_3)_3^g$ DAJVIT	11 738	<i>k</i>	+41.91, 1.02	-9.755, -2.05	[2.083, 2.087, 2.090]	[2.221, 2.314, 2.317]
$\text{CoCl}(\text{triphos})^h$ RUTTIJ	10 876	24,434 ^j	+2.48, 0.03	<i>m</i>	[2.050, 2.059, 2.061]	<i>m</i>
$\text{CoBr}(\text{NP3})^i$ CUWSIW	11,118	<i>k</i>	+12.69, 0.17	<i>m</i>	[2.076, 2.087, 2.088]	<i>m</i>

^aCrystallographic geometry used (CSD code: KOCVON⁹). ^bCrystallographic geometry for chlorido analogue used (KOVCON⁹), but with Cl replaced by F and Co–F distance set at 2.070 Å, a distance estimated from distances seen in structurally characterized monofluorido cobalt complexes as described in Tables S2 and S3 (Supporting Information). Given that this was not an authentic structure, no singlet energy calculation was made. ^cCrystallographic geometry for chlorido analogue used (KOCVON⁹), but with Cl replaced by Br and Co–Br distance set at 2.365 Å, the value found for $\text{CoBr}(\text{NP3})$.¹⁶ Given that this was not an authentic structure, no singlet energy calculation was made. ^dCrystallographic geometry for chlorido analogue used (KOCVON⁹), but with Cl replaced by I and Co–I distance set at 2.549 Å, the value found for $\text{CoI}(\text{PMe}_3)_3$.¹³ Given that this was not an authentic structure, no singlet energy calculation was made. ^eCrystallographic geometry used (CSD codes: BUTDEZ¹¹ and BUTDEZ01¹²). Hydrogen atoms were added to the structure for BUTDEZ. ^fCrystallographic geometry for chlorido analogue used (BUTDEZ01¹²), but with Cl replaced by Br and Co–Br distance set at 2.365 Å, the value found for $\text{CoBr}(\text{NP3})$ ¹⁶ and at 2.375 Å, the average of the Co–X distances found for X = Cl and I.¹³ ^gCrystallographic geometry used (CSD code: DAJVIT¹³). ^hCrystallographic geometry used (CSD code: RUTTIJ¹⁵). ⁱCrystallographic geometry used (CSD code: CUWSIW¹⁶). ^jThe sign of D was calculated to be positive (except for $\text{CoI}(\text{PMe}_3)_3$), in agreement with experiment and with LFT; the sign of E is assigned as to be the same as that of D by convention. ^kSinglet state energy calculation did not converge. ^lSinglet state energy calculation did converge, but the singlet–triplet difference is unreasonably large and spin Hamiltonian parameters could not be calculated. ^mNot calculated; the molecule size may have exceeded the software's capacity.

greater g anisotropy than is actually observed in integer spin systems⁶⁴), the ordering of g_{\perp} matches the ordering of D values, as seen experimentally. What is clear is that LFT shows that the structural differences among the three molecules are also reflected in the different sets of g matrices. Consequently, the calculated magnetic susceptibility behavior of the three molecules in $\text{CoCl}(\text{PPh}_3)_3$ is different, as also shown in Table 2, which uses the same parameters as the zfs calculation, additionally with the electronic Zeeman interaction, $\mathcal{H}_Z = \beta H \cdot (kL + g_s S)$, where $k = 0.52$ gives the best match with experiment. This represents a significant orbital reduction factor, consistent with a need for a low value for the SOC constant, ζ , described above.

Lastly, we predict that the crystal structure of $\text{CoBr}(\text{PPh}_3)_3$ will exhibit trigonal symmetry, but with three crystallographically distinct molecules per unit cell. However, the sensitivity of zfs on AOM bonding parameters and hence on structure means that it is pointless to apply the AOM to $\text{CoBr}(\text{PPh}_3)_3$ absent a crystal structure. Qualitatively, the chlorido and bromido complexes should give very similar results in terms of bonding parameters.

QCT Analysis. The first goal of the quantum chemical theory (QCT) calculations was to validate the simple LFT result that these pseudotetrahedral Co(I) complexes exhibit spin triplet ground states. Using DFT methods and $\text{CoCl}(\text{PMe}_3)_3$ as an initial case with both of the crystallographically

determined geometries,^{11,12} the program ORCA³⁹ gave a spin triplet state lower in energy than the singlet by $\sim 11\ 700\ \text{cm}^{-1}$. For the three crystallographically distinct molecules in $\text{CoCl}(\text{PPh}_3)_3$, the spin triplet was lower in energy by $\sim 12\ 000\ \text{cm}^{-1}$. These values can be compared to the LFT result for $\text{CoCl}(\text{PPh}_3)_3$, which gave the lowest singlet states at $\sim 8000\text{--}9000\ \text{cm}^{-1}$ above the triplet ground state. The same calculations were performed for analogous complexes: those with chelating ligands (triphos, NP3) and/or with other halido ligands (Br, I). The results are summarized in Table 4. The singlet–triplet splitting in all cases is roughly the same: $\sim 11\ 000\text{--}12\ 000\ \text{cm}^{-1}$.

DFT also provides graphical descriptions of the molecular orbitals in these systems. As an example, we show in Figure 7 the α spin form of each of the two semioccupied molecular orbitals (SOMOs) calculated for $S = 1$ $\text{CoBr}(\text{PMe}_3)_3$ using the structure of the chlorido analogue (CSD code: BUTDEZ01¹²), but with Cl replaced by Br and the Co–Br distance set at 2.365 Å, the value found for $\text{CoBr}(\text{NP3})$.¹⁶ Both SOMOs clearly show primarily Co 3d character as well as their Co–Br π^* nature.

DFT was also used to calculate the spin Hamiltonian parameters for $S = 1$: D , E/D , and the g matrix (see Table 4). The zfs calculated by DFT for $\text{CoCl}(\text{PR}_3)_3$ ($\text{R} = \text{Me}, \text{Ph}$) has the correct, positive sign, and is essentially axial, but the magnitude, in contrast to the result from LFT, is too small.

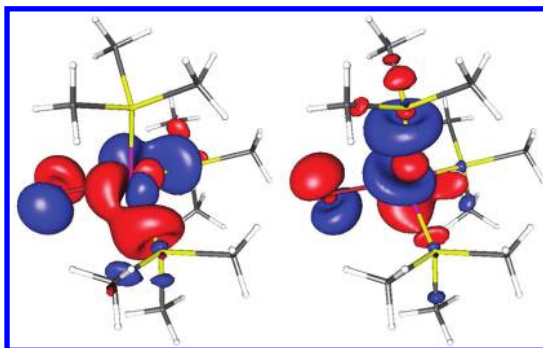


Figure 7. Depiction of α semioccupied molecular orbitals (SOMOs) calculated for $S = 1$ $\text{CoBr}(\text{PMe}_3)_3$ using the structure of the chlorido analogue,¹² with Cl replaced by Br at 2.365 Å, the Co–Br distance in $\text{CoBr}(\text{NP}3)$.¹⁶ Both SOMOs clearly show primarily Co 3d character and the π^* character of the Co–Br bond.

For $R = \text{Ph}$, $D \approx +1 \text{ cm}^{-1}$, off by nearly an order of magnitude for molecule 3. Moreover, although the differences among calculated D values are so small as to be perhaps insignificant, the largest zfs is calculated for molecule 2, for which LFT predicts the smallest zfs, corresponding to triplet C. For $R = \text{Me}$, for which we have no experimental data, $D = +2.2 \text{ cm}^{-1}$, which approaches with 50% of the value for molecule 1. A similar D value is calculated for $\text{CoCl}(\text{triphos})$. One might wonder if the lower lying singlet states calculated by LFT have an effect on the calculated zfs versus the results from QCT. This appears not to be the case. Use of a very large value for the Racah C parameter (10-fold the appropriate value), so that all of the singlet states are inaccessibly high in energy, leads to only a slight increase in calculated D : e.g., from $+5.66 \text{ cm}^{-1}$ to $+5.83 \text{ cm}^{-1}$ (for molecule 3).⁶⁵ It is also disturbing in QCT that, in only one case, $\text{CoCl}(\text{PMe}_3)_3$ (structure BUTDEZ01¹²) is an axial zfs calculated; in the other cases, despite the symmetry, $E \neq 0$ is calculated (see Table 4). Calculations for the complexes with chelating ligands lack the crystallographic 3-fold symmetry of $\text{CoCl}(\text{PR}_3)_3$ ($R = \text{Me, Ph}$), and slightly rhombic zfs is calculated and expected. Essentially axial g values are calculated, and with $g > g_s$, as expected, but the deviation from 2.00 is much less than expected, consistent with the calculated D being too low in magnitude. Use of different basis sets for the heavy atoms has only a slight effect on zfs calculations: TZVPP for Co, P, and Cl in $\text{CoCl}(\text{PMe}_3)_3$ (structure BUTDEZ) gives $D = +2.301 \text{ cm}^{-1}$, while only TZV gave $D = +2.190 \text{ cm}^{-1}$. The halido ligand appears to have a large effect; however, with D values calculated for $\text{CoBr}(\text{NP}3)$ and *ersatz* $\text{CoBr}(\text{PMe}_3)_3$ (i.e., use of the structure for the chlorido complex with Cl replaced by Br at each of two viable bond lengths) being $\sim 13\text{--}14 \text{ cm}^{-1}$, significantly larger than experiment. The situation for the iodido complexes, both authentic ($\text{CoI}(\text{PMe}_3)_3$)¹³ and *ersatz* ($\text{CoI}(\text{PPh}_3)_3$ generated by replacement of Cl by I at the bond length of the PMe_3 complex), is even more striking, with calculated $D = +42 \text{ cm}^{-1}$. Were this the case, then HFEPR of $\text{CoI}(\text{PPh}_3)_3$ would likely be unsuccessful. Clearly, DFT suggests a strong effect of halido ligand on zfs, which we have seen experimentally in other systems, namely, Tp^*NiX ($\text{Tp}^* = \text{tris}(3,5\text{-dimethylpyrazolyl})\text{borate}$, $X = \text{Cl, Br, I}$).⁴⁷ We have explored this effect further by generation of an *ersatz* fluorido complex, $\text{CoF}(\text{PPh}_3)_3$, created by replacement of the Cl of $\text{CoCl}(\text{PPh}_3)_3$ molecule 1⁹ by F. The choice of Co–F bond length is challenging. We surveyed the CSD (update 5.32) and found a few relevant examples in which Co (as

Co(II) or more commonly Co(III)) had a single fluorido ligand and a coordination sphere that otherwise somewhat resembled the hypothetical complex. A list of such complexes is given in Table S2 (Supporting Information), which shows that the Co–F distance does not vary greatly ($1.94 \pm 0.04 \text{ \AA}$). We then looked at the series of complexes $\text{Tp}^{\text{R'R}}\text{CoX}$ ($X = \text{F, Cl, I}$; there is no Br complex), for which the data are summarized in Table S3 (Supporting Information). This information in combination with the Co–X bond lengths in authentic $\text{CoX}(\text{PR}_3)_3$ complexes (Table S1) suggests that a reasonable Co–F bond length for $\text{CoF}(\text{PR}_3)_3$ is 2.07 Å. DFT gives a very small magnitude zfs for this complex, qualitatively similar to the results for the chlorido complexes.

UHF methods were also employed, since in other 3d⁸ systems they gave some of us much better results than DFT,⁶⁶ although UHF is inferior compared to *ab initio* methods. In several cases, however, the molecules studied here were too complex for the ORCA program to converge and/or give results in any reasonable length of time (see Table 4). In particular, it was not possible to calculate singlet energies successfully; however, this not a concern since the molecules so clearly exhibit spin triplet ground states. Nevertheless, the $S = 1$ results for one of the simpler systems, $\text{CoCl}(\text{PMe}_3)_3$ (structure BUTDEZ01¹²), are very promising in that an axial zfs is calculated with magnitude seemingly appropriate for these systems. The calculated g matrix is also quite reasonable, in contrast to the results from DFT as mentioned above. The parameters calculated for the bromido complexes also appear to be more plausible by UHF as opposed to DFT.

QCT also gives some insight into the various contributions to zfs. We shall focus on the UHF calculations for $\text{CoX}(\text{PPh}_3)_3$ since these are the most relevant to experiment and give overall the best results. As seen in Supporting Information (sections 5–8, and summarized in section 9), the dominant, and positive, SOC contribution to D (D^{SOC} for $X = \text{F, Cl, Br}$; $X = \text{I}$ is different as described below) is from same-spin transitions from filled to partly filled orbitals ($\text{DOMO } \beta \rightarrow \text{SOMO } \beta$), but there is a smaller magnitude, negatively signed contribution from spin-flip transitions from partly filled to partly filled MOs ($\text{SOMO } \alpha \rightarrow \text{SOMO } \beta$). The relative magnitudes of these two contributions could each be slightly altered by the changes in MO energies reflected in the structural differences seen for the three molecules in $\text{CoCl}(\text{PPh}_3)_3$ and presumably the bromido complex, and lead to the three sets of zfs parameters for each. The UHF calculations also suggest that the contribution to zfs from SSC (D^{SSC}) is very small, ca. 1% of D for the chlorido complex (0.13 cm^{-1}) and generally less (in relative and absolute terms) for the heavier halides. Thus, the difficulties with LFT are likely not the consequence of neglecting SSC.^{67–69}

The UHF calculations do give a hint as to the ligand contribution described above. Interestingly, these give a negative value for D for the authentic (PMe_3) iodido complex, although not for the *ersatz* (PPh_3) complex. We can see a rough trend in calculated D (in cm^{-1}) for the series $\text{CoX}(\text{PR}_3)_3$: $R = \text{Me}$ (BUTDEZ01), $X = \text{Cl, Br, I}$ ($+10.2, +5.8, -9.8$); $R = \text{Ph}$ (KOCVON molecule 1), $X = \text{F, Cl, Br, I}$ ($+20.8, +10.3, +14.4, +30.3$).⁷⁰ The first point is that the zfs in an iodido complex in particular is unpredictable, likely due to its own SOC effects. This has already been shown for a Mn(III) diiodido complex.⁶⁰ The second point is that for the putative fluorido complex, for which one would expect the smallest contribution from SOC

involving the ligand, the zfs magnitude is closer to that expected using LFT.⁷¹

One can also compare the contribution to the overall D value (in cm^{-1}) from transitions from SOMOs and DOMOs to virtual MOs (VMOs) in the $\text{CoX}(\text{PPh}_3)_3$ series: (SOMO \rightarrow VMO) F, -0.30 ; Cl, -0.06 ; Br, $+3.5$; I, $+19.1$; (DOMO \rightarrow VMO) F, $+0.07$; Cl, -0.04 ; Br, -0.52 ; I, -4.16 . These data show a clear periodic trend that suggests the complexity of the heavy atom halido ligand in ways that could not be easily modeled with LFT. We believe that more advanced QCT methodology, such as has been applied by Neese and co-workers in other systems,^{68,72–74} will be needed to model fully the electronic structure of these pseudotetrahedral phosphine/halide complexes of Co(I).

CONCLUSIONS

The synthesis of the spin triplet Co(I) complexes, $\text{CoX}(\text{PPh}_3)_3$, where X = Cl, Br, I, was reported many years ago.⁸ The most accessible member of the series, the Cl complex, has growing uses in organic synthesis as a radical coupling reagent.^{26–28} The crystal structure of the chlorido complex was also reported, and showed crystallographic 3-fold symmetry, but with three distinct molecules per unit cell.⁹ We have used HFEPR to study the Cl and Br complexes, which show rigorously axial spin triplet spectra, in agreement with the symmetry of the chlorido complex; we propose that this symmetry is also obtained for the bromido complex. We have used LFT to analyze quantitatively the electronic absorption spectra of all three complexes. The combination of this analysis with HFEPR shows that the Cl and Br, and likely I, complexes have a ${}^3\text{A}_2[{}^3\text{T}_1(\text{F})]$ electronic ground state (C_{3v} symmetry). Our current analysis shows similar, but weaker, bonding interactions than in analogous Ni(II) complexes, and can also reproduce the positive sign of the axial zfs (D value), determined by HFEPR. However, a surprisingly low value of the SOC constant (ζ) is needed to reproduce the magnitude of D . Nevertheless, use of the AOM shows that the slight structural differences among the three molecules per unit cell can be manifest in three sets of zfs parameters, which is seen experimentally in that three distinct spin triplets are observed. The magnitude of differences among these triplets corresponds to that from LFT. QCT calculations, both DFT and UHF, were also used on the molecules studied and on related systems, including models. The results were in qualitative agreement with experiment; however, DFT underestimated the zfs, while UHF overestimated it. DFT and UHF methods are unreliable for quantitative purposes, but may be helpful in showing trends for a defined series such as $\text{CoX}(\text{PR}_3)_3$ (X = group 17 ions). Analysis of the results shows the crucial role of the halido ligand in producing the overall zfs. More advanced quantum chemical calculations, using *ab initio* techniques, will be necessary to unravel the zfs effects in these complexes. Overall, however, this study demonstrates the detailed information on electronic structure, on a relatively poorly studied ion, that can be derived from HFEPR in conjunction with other spectroscopic and structural data, in conjunction with LFT and QCT. We hope that this work will inspire further study of HS Co(I), such as in novel complexes with interesting reactivity.⁵

ASSOCIATED CONTENT

Supporting Information

Table of metric data of Co(I) complexes; figures showing the effect of air exposure on solution absorption spectrum of $\text{CoBr}(\text{PPh}_3)_3$ and solid reflectance spectrum of $\text{CoCl}(\text{PPh}_3)_3$; two representative Ligfield output files; two representative, complete ORCA input/output files and four output files. This material is available free of charge via the Internet at <http://pubs.acs.org>.

AUTHOR INFORMATION

Corresponding Author

*E-mail: jtelsler@roosevelt.edu.

Notes

The authors declare no competing financial interest.

ACKNOWLEDGMENTS

This work has been supported by the NHMFL, which is funded by the NSF (Cooperative Agreement DMR 0654118), State of Florida, and DOE. Additional NHMFL funding (User Collaboration Grant 5062, J.K. and J.T.) is acknowledged. The UV-vis-NIR spectrophotometer at Roosevelt University was funded by the Goldenberg Foundation and the glovebox by DOE. S.A.Z. acknowledges the support of the Deutsche Forschungsgemeinschaft and EuroMagNET II. We thank Professors James A. Larabee (Middlebury College) and Gerard Parkin (Columbia University) for helpful comments and Professor Jesper Bendix (Copenhagen University, Denmark) for the program Ligfield.

REFERENCES

- (1) Cotton, F. A.; Wilkinson, G.; Murillo, C. A.; Bochmann, M. In *Advanced Inorganic Chemistry*, 6th ed.; John Wiley & Sons, Inc.: New York, 1999.
- (2) Banerjee, R.; Ragsdale, S. W. *Annu. Rev. Biochem.* **2003**, *72*, 209–247.
- (3) Staeb, T. H.; Chávez, J.; Gleiter, R.; Nuber, B. *Eur. J. Inorg. Chem.* **2005**, 4090–4093.
- (4) O'Hare, D.; Rai-Chaudhuri, A.; Murphy, V. *J. Chem. Soc., Dalton Trans.* **1993**, 3071–3074.
- (5) Dugan, T. R.; Sun, X.; Rybak-Akimova, E. V.; Olatunji-Ojo, O.; Cundari, T. R.; Holland, P. L. *J. Am. Chem. Soc.* **2011**, *133*, 12418–12421.
- (6) Whitfield, J. M.; Watkins, S. F.; Tupper, G. B.; Baddley, W. H. *J. Chem. Soc., Dalton Trans.* **1977**, 407–413.
- (7) Choi, H.; Park, S. *Chem. Mater.* **2003**, *15*, 3121–3124.
- (8) Aresta, M.; Rossi, M.; Sacco, A. *Inorg. Chim. Acta* **1969**, *3*, 227–231.
- (9) Cassidy, J. M.; Whitmire, K. H. *Acta Crystallogr.* **1991**, *C47*, 2094–2098.
- (10) Klein, H. F.; Karsch, H. H. *Inorg. Chem.* **1975**, *14*, 473–477.
- (11) Jones, R. A.; Stuart, A. L.; Atwood, J. L.; Hunter, W. E. *J. Chem. Crystallogr.* **1983**, *13*, 273–278.
- (12) Dai, C.; Stringer, G.; Corrigan, J. F.; Taylor, N. J.; Marder, T. B.; Norman, N. C. *J. Organomet. Chem.* **1996**, *513*, 273–275.
- (13) Bandy, J. A.; Green, J. C.; Kirchner, O. N. *Acta Crystallogr.* **1985**, *C41*, 1179–1181.
- (14) Sacconi, L.; Midollini, S. *J. Chem. Soc., Dalton Trans.* **1972**, 1213–1216.
- (15) Heinze, K.; Huttner, G.; Zsolnai, L.; Schober, P. *Inorg. Chem.* **1997**, *36*, 5457–5469.
- (16) Ghilardi, C. A.; Mealli, C.; Midollini, S.; Orlandini, A. *Inorg. Chem.* **1985**, *24*, 164–168.
- (17) Krzystek, J.; Ozarowski, A.; Telser, J. *Coord. Chem. Rev.* **2006**, *250*, 2308–2324.

(18) Krzystek, J.; Zvyagin, S. A.; Ozarowski, A.; Trofimenko, S.; Telser, J. *J. Magn. Reson.* **2006**, *178*, 174–183.

(19) Abbreviations used: AOM, angular overlap model; DFT, density functional theory; DOMO, doubly occupied molecular orbital; HFEPR, high-frequency and -field electron paramagnetic resonance; HS, high-spin; LFT, ligand-field theory; LS, low-spin; NP3, tris(2-(diphenylphosphino)ethyl)amine; QFT, quantum chemical theory; SOC, spin–orbit coupling; SOMO, singly (or semi) occupied molecular orbital; SSC, spin–spin coupling; triphos, 1,1,1-tris((diphenylphosphino)methyl)ethane; UHF, unrestricted Hartree–Fock; VMO, virtual molecular orbital; zfs, zero-field splitting.

(20) Krzystek, J.; Zvyagin, S. A.; Ozarowski, A.; Fiedler, A. T.; Brunold, T. C.; Telser, J. *J. Am. Chem. Soc.* **2004**, *126*, 2148–2155.

(21) Krzystek, J.; Park, J.-H.; Meisel, M. W.; Hitchman, M. A.; Stratemeier, H.; Brunel, L.-C.; Telser, J. *Inorg. Chem.* **2002**, *41*, 4478–4487.

(22) Vongtragool, S.; Gorshunov, B.; Dressel, M.; Krzystek, J.; Eichhorn, D. M.; Telser, J. *Inorg. Chem.* **2003**, *42*, 1788–1790.

(23) Kawakami, K.; Mizoroki, T.; Ozaki, A. *Bull. Chem. Soc. Jpn.* **1978**, *51*, 21–24.

(24) Kawakami, K.; Mizoroki, T.; Ozaki, A. *J. Mol. Catal.* **1979**, *5*, 175–187.

(25) Yamada, Y.; Momose, D.-i. *Chem. Lett.* **1981**, *10*, 1277–1278.

(26) Movassaghi, M.; Schmidt, M. A. *Angew. Chem., Int. Ed.* **2007**, *46*, 3725–3728.

(27) Bagal, S. K.; Adlington, R. M.; Marquez, R.; Cowley, A. R.; Baldwin, J. E. *Tetrahedron Lett.* **2003**, *44*, 4993–4996.

(28) Bagal, S. K.; Adlington, R. M.; Baldwin, J. E.; Marquez, R. *J. Org. Chem.* **2004**, *69*, 9100–9108.

(29) Cotton, F. A.; Faut, O. D.; Goodgame, D. M. L.; Holm, R. H. *J. Am. Chem. Soc.* **1961**, *83*, 1780–1785.

(30) Krzystek, J.; Swenson, D. C.; Zvyagin, S. A.; Smirnov, D.; Ozarowski, A.; Telser, J. *J. Am. Chem. Soc.* **2010**, *132*, 5241–5253.

(31) Figure 1 in Aresta et al.⁸ shows structured features at 600–700 nm that we strongly suspect are due to contamination by Co(II), by analogy with spectra of authentic, trigonally distorted four-coordinate Co(II) complexes that we have studied.³⁰

(32) Hassan, A. K.; Pardi, L. A.; Krzystek, J.; Sienkiewicz, A.; Goy, P.; Rohrer, M.; Brunel, L.-C. *J. Magn. Reson.* **2000**, *142*, 300–312.

(33) Abragam, A.; Bleaney, B. *Electron Paramagnetic Resonance of Transition Ions*; Dover Publications, Inc.: Mineola, NY, 1986.

(34) Ballhausen, C. J. In *Introduction to Ligand Field Theory*; McGraw-Hill: New York, 1962; pp 99–103.

(35) Schäffer, C. E. *Struct. Bonding (Berlin)* **1968**, *5*, 68–95.

(36) Figgis, B. N.; Hitchman, M. A. *Ligand Field Theory and its Applications*; Wiley-VCH: New York, 2000.

(37) Bendix, J.; Brorson, M.; Schäffer, C. E. *Inorg. Chem.* **1993**, *32*, 2838–2849.

(38) Brorson, M.; Schäffer, C. E. *Inorg. Chem.* **1988**, *27*, 2522–2530.

(39) Neese, F. ORCA—An *Ab Initio*, Density Functional and Semiempirical Program Package, 2.8.0; Universität Bonn: Bonn, Germany, 2010.

(40) Schäfer, A.; Horn, H.; Ahlrichs, R. *J. Chem. Phys.* **1992**, *97*, 2571–2577.

(41) Eichkorn, K.; Treutler, O.; Öhm, H.; Häser, M.; Ahlrichs, R. *Chem. Phys. Lett.* **1995**, *240*, 283–289.

(42) Eichkorn, K.; Weigend, F.; Treutler, O.; Ahlrichs, R. *Theor. Chem. Acc.* **1997**, *97*, 119–124.

(43) Becke, D. A. *Phys. Rev. A* **1988**, *38*, 3098–3100.

(44) Weigend, F.; Ahlrichs, R. *Phys. Chem. Chem. Phys.* **2005**, *7*, 3297–3305.

(45) Zheng, B.; Miranda, M. O.; DiPasquale, A. G.; Golen, J. A.; Rheingold, A. L.; Doerr, L. H. *Inorg. Chem.* **2009**, *48*, 4274–4276.

(46) The zfs is inversely proportional to the trigonal splitting, $D \propto \lambda^2/\Delta$, so that a larger magnitude of D_s allows a larger value for ζ , approaching 50% of the free-ion value.

(47) Desrochers, P. J.; Telser, J.; Zvyagin, S. A.; Ozarowski, A.; Krzystek, J.; Vicić, D. A. *Inorg. Chem.* **2006**, *45*, 8930–8941.

(48) Nieto, I.; Bontchev, R. P.; Ozarowski, A.; Smirnov, D.; Krzystek, J.; Telser, J.; Smith, J. M. *Inorg. Chim. Acta* **2009**, *362*, 4449–4460.

(49) Davies, J. E.; Gerloch, M.; Phillips, D. J. *J. Chem. Soc., Dalton Trans.* **1979**, 1836–1842.

(50) Gerloch, M.; Hanton, L. R. *Inorg. Chem.* **1981**, *20*, 1046–1050.

(51) Gerloch, M.; Manning, M. R. *Inorg. Chem.* **1981**, *20*, 1051–1056.

(52) Even with π -bonding, the 3E ground state is still obtained if ideal tetrahedral symmetry is used, rather than the real geometry.

(53) Sinnecker, S.; Neese, F. *J. Phys. Chem. A* **2006**, *110*, 12267–12275.

(54) Neese, F. *J. Am. Chem. Soc.* **2006**, *128*, 10213–10222.

(55) Ganyushin, D.; Gilka, N.; Taylor, P. R.; Marian, C. M.; Neese, F. *J. Chem. Phys.* **2010**, *132*, 144111.

(56) Malli, G.; Fraga, S. *Theor. Chim. Acta* **1967**, *7*, 80–84.

(57) Fraga, S.; Malli, G. *Many-Electron Systems: Properties and Interactions*; Saunders: Philadelphia, 1968.

(58) Ralchenko, Y.; Kramida, A. E.; Reader, J. *NIST ASD Team, NIST Atomic Spectra Database (ver. 4.1.0)*; National Institute of Standards and Technology: Gaithersburg, MD, 2011; <http://www.nist.gov/pml/data/asd.cfm>.

(59) These sources^{56–58} give the following ζ values (in cm^{-1} ; note that atomic P is 4S , which has no intraterm SOC): P^- , 194; P^+ , 303.8; F^* , 269.3; Cl^* , 587.3; Br^* , 2456.7; I^* , 5069.

(60) Mossin, S.; Weihe, H.; Barra, A.-L. *J. Am. Chem. Soc.* **2002**, *124*, 8764–8765.

(61) Ye, S.; Neese, F. Personal communication.

(62) Larrabee, J. A.; Johnson, W. R.; Volwiler, A. S. *Inorg. Chem.* **2009**, *48*, 8822–8829.

(63) Lever, A. B. P.; Walker, I. M.; McCarthy, P. J.; Mertes, K. B.; Jircitano, A.; Sheldon, R. *Inorg. Chem.* **1983**, *22*, 2252–2258.

(64) Krzystek, J.; England, J.; Ray, K.; Ozarowski, A.; Smirnov, D.; Que, L. Jr.; Telser, J. *Inorg. Chem.* **2008**, *47*, 3483–3485.

(65) Use of both B and C 10-fold the appropriate values, so that only the 3F term is considered, gives a decrease in calculated D : e.g., from $+5.66 \text{ cm}^{-1}$ to $+3.28 \text{ cm}^{-1}$ (for molecule 3), indicating the proportionately large, positive contribution of the 3P term to zfs.

(66) Wojciechowska, A.; Daszkiewicz, M.; Staszak, Z.; Truszczyński, A.; Bieńko, A.; Ozarowski, A. *Inorg. Chem.* **2011**, *50*, 11532–11542.

(67) The ORCA software provides two methods of calculating the SSC contribution, direct and UNO (UHF normal orbital); when compared here, these methods give D^{SSC} differing only modestly, e.g., for $\text{CoF}(\text{PMe}_3)_3$, $D^{\text{SSC}} = 0.28$ (direct), 0.61 cm^{-1} (UNO). This difference is too small to be significant, but gives an idea as to an “error bar” of these SSC calculations.

(68) Ganyushin, D.; Neese, F. *J. Chem. Phys.* **2006**, *125*, 024103.

(69) Ganyushin, D.; Neese, F. *J. Chem. Phys.* **2008**, *128*, 114117.

(70) DFT calculations for $\text{R} = \text{Ph}$ also show a clear trend in calculated D (in cm^{-1}), $\text{X} = \text{F}, \text{Cl}, \text{Br}, \text{I}$ (+0.08, +1.0, +11.9, +42.3); however, the magnitudes are even further from experiment than for UHF.

(71) The D value calculated here by UHF would be reproduced with the LFT parameters for the chlorido complex and $\zeta = 160 \text{ cm}^{-1}$, as opposed to 100 cm^{-1} ; we do not try to imagine bonding parameters for $\text{CoF}(\text{PPh}_3)_3$.

(72) Zein, S.; Neese, F. *J. Phys. Chem. A* **2008**, *112*, 7976–7983.

(73) Ye, S.; Neese, F.; Ozarowski, A.; Smirnov, D.; Krzystek, J.; Telser, J.; Liao, J.-H.; Hung, C.-H.; Chu, W.-C.; Tsai, Y.-F.; Wang, R.-C.; Chen, K.-Y.; Hsu, H.-F. *Inorg. Chem.* **2010**, *49*, 977–988.

(74) Desrochers, P. J.; Sutton, C. A.; Abrams, M. L.; Ye, S.; Neese, F.; Telser, J.; Ozarowski, A.; Krzystek, J. *Inorg. Chem.* **2012**, *51*, 2793–2805.

■ NOTE ADDED AFTER ASAP PUBLICATION

This paper was published on the Web on April 6, 2012, with minor errors in Table 4. The corrected version was reposted on April 13, 2012.